

Sertraline Racemate and Enantiomer: Solid-State Characterization, Binary Phase Diagram, and Crystal Structures

Quan He, Sohrab Rohani,* Jesse Zhu, and Hassan Gomaa

Department of Chemical and Biochemical Engineering, The University of Western Ontario London, Ontario, N6G 4R3, Canada

Received September 29, 2009; Revised Manuscript Received January 22, 2010

ABSTRACT: The racemate and enantiomer of sertraline free base were prepared and characterized. The crystalline sertraline enantiomer is relatively less polymorphic compared with the sertraline-HCl salt. The solid-state nature of sertraline racemate was identified to be a racemic compound through a binary melting point phase diagram and spectroscopy analysis. The crystal structures of the racemate and enantiomer were determined to be monoclinic $P12_1/n1$ and $P2_1$, respectively.

1. Introduction

Sertraline is one of the selective serotonin reuptake inhibitors (SSRI) that has been shown to be effective in the treatment of major depression. It may also be used for panic disorder, social phobia, obesity, or obsessive-compulsive disorder (OCD). Its chemical name is *(1S,4S)*-4-(3,4-dichlorophenyl)-1,2,3,4-tetrahydro-*N*-methyl-1-naphthalene-amine.¹ The structures of sertraline racemate and enantiomers are shown in Scheme 1.

Sertraline is marketed in the form of its hydrochloride salt, brand name Zoloft, which is one of the most highly polymorphic salts known today. Up to now 28 polymorphic crystalline forms of sertraline HCl have been disclosed in patents,² including pure salt forms, hydrates, and solvates. Therefore, much effort has been made to obtain single polymorph since it is desirable to control the specific form and avoid a mixture of several forms for formulations of the active pharmaceutical ingredient (API).³ A critical polymorphic analysis of other salt forms demonstrated that seemingly minor differences in salt former can have profound unpredictable effects on the number of polymorphs and solvates.^{4–6} For example, the sertraline bromide was found to be much less polymorphic than sertraline chloride.⁵ Since there is currently no accurate method to predict the polymorphic behavior of a given solid form (e.g., a salt or cocrystal vs free base/acid), extensive experimentation is needed for screening polymorphs in the early stage. Thus, it may be possible to find a proper solid form with less polymorphic propensity and make formulation, manufacture, and storage more reliable, robust, and cost-effective.^{7,8}

There are several forms of solid-state API including the drug free acid/base, neutral molecules, solvates, salts, or cocrystals. The choice and design of the preferred solid form is based on the comparison of each form's physicochemical properties (solubility, bioavailability, hygroscopicity, melting point, dissolution rate, and stability) as well as the required properties for dosage and drug delivery.⁹ Salt forms are frequently used in formulations due to their advantages including modified solubility, improved physical and chemical stabilities, masked unpleasant taste, increased bioavailability,

and enhanced manufacturability. However, in some cases, the free base/acid is a better choice especially when API has a low pK_a value and the resulting salts are less stable or more hygroscopic or when they exhibit complex polymorphism/pseudopolymorphism.^{8,9} Exploring other possible solid forms than the currently used sertraline HCl salt for drug development is therefore a worthwhile attempt.

Additionally, the present manufacturing process of enantiomerically pure sertraline involves a classical resolution via diastereomeric salt crystallization, in which (*R*)-mandelic acid is introduced as a resolving agent to form the less soluble *(1S,4S)*-sertraline mandelate. Subsequently, the single enantiomer sertraline free base *(1S,4S)*-sertraline is isolated from mandelate and converted into its hydrochloride.¹⁰ The classical resolution by diastereomeric salt formation has many advantages such as the simplicity of crystallization operation, the ease of process scale-up, and the availability of both enantiomers.¹¹ However, the process involves many steps. Very often, several recrystallization steps are needed to achieve high optical purity. Moreover, the intermediate diastereomeric salt has to be decomposed resulting in the desired enantiomer and recovery of the resolving agent. Thus, development of other more efficient chiral separation techniques has been of great interest to both the pharmaceutical industry and academic researchers. Other possible separation methods without introducing foreign chiral agents such as direct crystallization, enrichment crystallization, and coupling crystallization with other separation processes are very attractive.

The specific method that can be applied depends on the solid nature of a given racemate which is basically classified into conglomerate, racemic compound, or pseudoracemate (solid solution).¹² The determination of the solid nature of a certain racemate is the prerequisite for rational design of chiral resolution and purification process of pharmaceuticals. It can provide a valuable thermodynamic basis for chiral separation, chiral enrichment, and chiral purification.¹³ For example, if racemate belongs to the conglomerate, direct crystallization will be applied.¹⁴ If it is a racemic compound, the chiral purification by crystallization can be employed as long as the enantiomeric excess (ee) of the starting mixture enriched with the desired enantiomer provided by asymmetric synthesis, simulated moving bed (SMB) chromatography or other

*To whom correspondence should be addressed. E-mail: rohani@eng.uwo.ca.

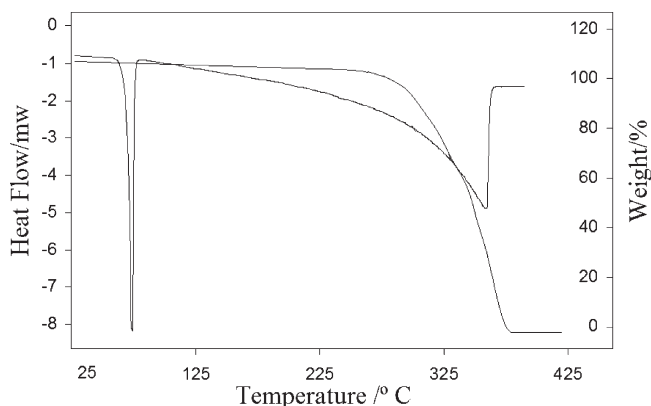
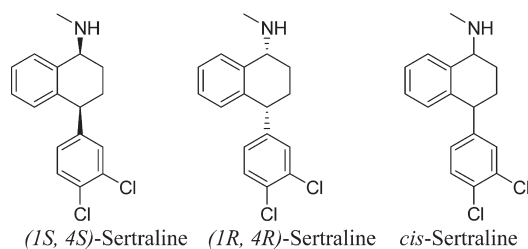


Figure 1. DSC and TGA of sertraline enantiomer.

Scheme 1. Structures of Sertraline Racemate and Enantiomer



method exceeds the ee of eutectic point of racemate.¹⁵ In order to identify the solid-state nature of racemate, establishment of a binary phase diagram by measuring the melting behavior of the mixtures with different enantiomeric compositions is commonly used.^{16–19}

In the present work, we prepared the sertraline enantiomer base as a crystalline form, characterized its physical properties, and performed a preliminary polymorphs screening. The sertraline enantiomer base is a potential alternative for pharmaceutical formulations instead of sertraline salts. The advantages of using the free base for formulation lies in that the free base is less polymorphic and can be further purified by crystallization during the preparation process. Second, we also obtained crystalline sertraline racemate base, namely, *racis*-4-(3,4-dichlorophenyl)-1,2,3,4-tetrahydro-*N*-methyl-1-naphthaleneamine (a mixture of equal $(1R,4R)$ - and $(1S,4S)$ -enantiomer). Thus, a binary melting point phase diagram of the mixture of sertraline enantiomers on the basis of thermoanalytical data was established. The solid-state nature of sertraline racemate was identified to be a racemic compound. The eutectic point was at $X_e = 0.84$ (the molar fraction of $(1S,4S)$ -sertraline enantiomer) and T_e (melting point of eutectic composition) was 58 °C. Finally, crystal structures of sertraline racemate and enantiomer were obtained and compared to each other, which demonstrated that sertraline racemate could exist as a stable racemic compound. The solid-state nature investigation of sertraline provides valuable thermodynamic basis for exploring other possible separation methods rather than classical resolution and the possibility of chiral purification by direct crystallization.

2. Experimental Section

2.1. General. Sertraline enantiomer and sertraline racemate hydrochloride salts were donated by Apotex PharmaChem Inc. (Canada). All solvents were HPLC grade and were used without further purification.

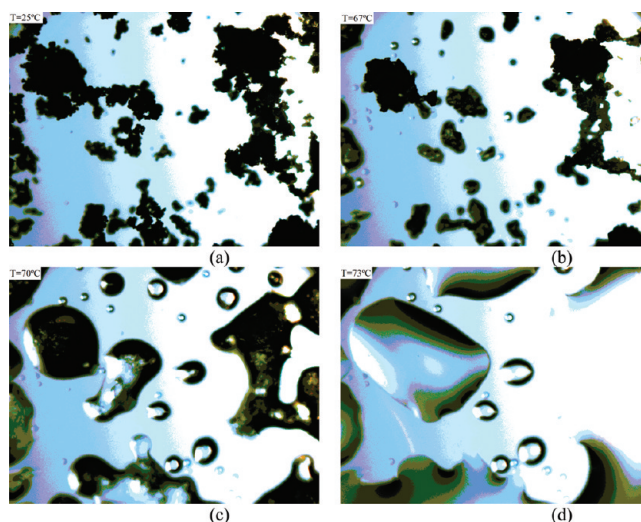


Figure 2. Hot stage micrographs of sertraline enantiomer. (a) $T = 25$ °C; (b) $T = 67$ °C; (c) $T = 70$ °C; (d) $T = 73$ °C.

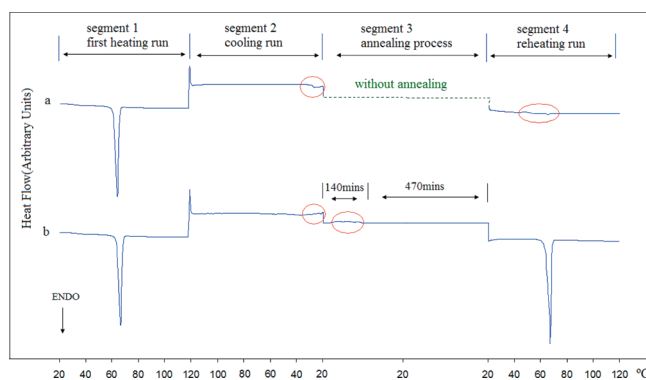


Figure 3. DSC traces of sertraline enantiomer under heat-cool-heat cycle.

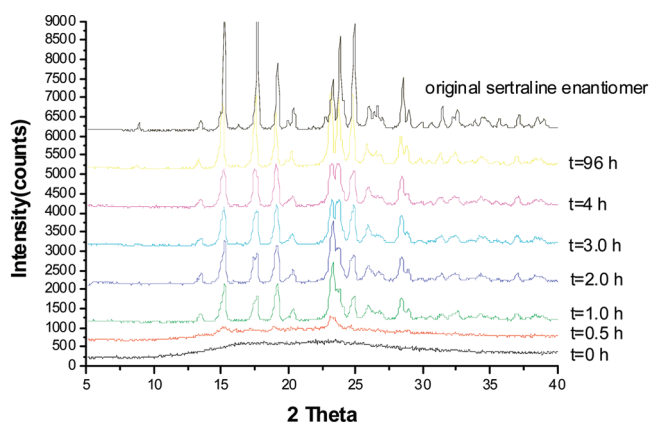


Figure 4. XRPD patterns of solid crystallized from the melt of sertraline enantiomer.

¹H NMR experiments were performed on a Varian INOVA 600 spectrometer at 25 °C and DMSO-*d*₆ as solvent. The X-ray powder diffraction (XRPD) spectra were collected on a Rigaku-Miniflex powder diffractometer (Carlsbad, CA) using CuK α (λ for K $\alpha = 1.54059$ Å) radiation obtained at 30 kV and 15 mA. The scans were run from 5.0° to 40.0° 2θ , increasing at a step size of 0.02° 2θ with a counting time of 5 s for each step. Specific rotations of salts were measured by Autopol IV Digital Polarimeter Rudolph America (Hackettstown, NJ) at 589 nm, equipped with a quartz cell of

100 mm path length. Solid-state FTIR spectra were recorded with a Fourier transformation infrared spectrometer (Bruker Vector 22, Billerica, MA) equipped with OPUS v3.1. The samples were analyzed by FTIR in transmittance mode through a diamond window. The number of scans was 32 over the 600 to 4000 cm^{-1} spectral region with a resolution of 4 cm^{-1} . The background was collected in the same range for air. Hygroscopicity was measured on dynamic vapor sorption (DVS) Advantage-1 system (Surface Measurement Systems Ltd., Alperton, Middlesex, UK). Approximate 100 mg samples were weighed into the sample pan and exposed to water partial pressure (p/p_0) cycle of 0–90%. Equilibrium at each step was determined by a dm/dt of 0.0005%/min. Melting behavior and other thermal transition of solid samples were investigated by Lincam LTS350 hot stage equipped by Lincam TNS 94 programmable heater and a ZEISS microscope.

2.2. Preparation and Characterization of Sertraline Base. Enantiomer.

(1*S*,4*S*)-(+)-4-(3,4-Dichlorophenyl)-1,2,3,4-tetrahydro-*N*-

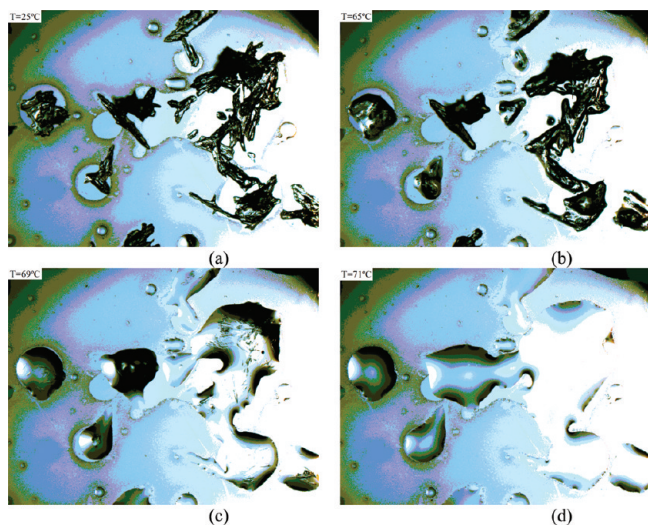


Figure 5. HSM of sertraline enantiomer crystallized from melt. (a) $T = 25\text{ }^{\circ}\text{C}$; (b) $T = 65\text{ }^{\circ}\text{C}$; (c) $T = 69\text{ }^{\circ}\text{C}$; (d) $T = 71\text{ }^{\circ}\text{C}$.

Table 1. Solubilities of Sertraline Enantiomer Free Base and Its Salts

	solubility mg/mL	melting point $^{\circ}\text{C}$
free base ^a	0.13	65.87
free base ^b	< 0.1	
hydrochloride ^b	3.8	249
hydrobromide ^c	0.6	266
<i>p</i> -toluenesulfonate ^c	0.1	265
lactate ^c	1.9	150
methanesulfonate ^c	4.2	201
benzenesulfonate ^c	0.3	150

^a Solubility was measured at room temperature in deionized water; the pH value of saturated solution at dissolution equilibrium is 7.66, the $\text{p}K_{\text{a}}$ value of sertraline free base is 9.5 from ref 6. ^b Data are from ref 6. ^c Data are from ref 5.

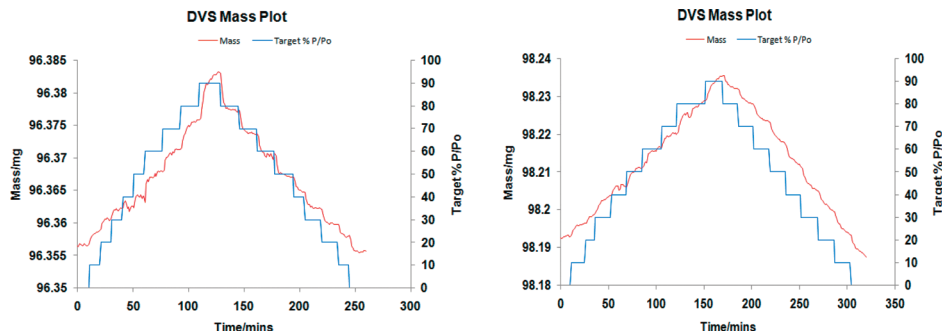


Figure 6. DVS profiles of sertraline enantiomer (left) and sertraline HCl (right).

methyl-1-naphthalenamine hydrochloride (6.8 g, 0.02 mol) was suspended in NaOH aqueous solution (50 mL, 5 N) and ethyl acetate (50 mL) was gradually added. The mixture was stirred until two phases became clear. The organic phase was separated from the water phase and dried over Na_2SO_4 . The ethyl acetate was removed in vacuo and oily free base was obtained. Hexane (10 mL) was added and heated to 50 $^{\circ}\text{C}$. When cooled to room temperature, the solution became cloudy. The solution was further cooled to 4 $^{\circ}\text{C}$ and white crystals formed. Crystals were filtered off and dried at room temperature overnight in vacuo to give sertraline free base 4.8 g (yield: 77%).

Melting point: 65.58–67.25 $^{\circ}\text{C}$ (onset of DSC). Specific rotation $[\alpha]_{\text{D}}^{15} = +59.8^{\circ}$ ($c = 1$, methanol). ^1H NMR (DMSO- d_6 /TMS), δ (ppm): 1.67–1.72 (m, H), 1.87–1.94 (m, 2H), 1.96 (s, 1H), 2.00–2.06 (m, H), 2.35 (s, 3H), 3.61 (d, 1H), 4.08 (t, 1H), 6.69 (d, 1H), 7.08 (t, 1H), 7.14–7.17 (m, 2H), 7.375 (d, 1H), 7.405 (d, 1H), 7.545 (d, 1H). IR $\nu(\text{cm}^{-1})$: 2937(w), 2846(w), 2778(w), 1735(s), 1469(s), 1363(s), 1214(s), 1126(s), 1027(s).

Racemate. *cis*-4-(3,4-Dichlorophenyl)-1,2,3,4-tetrahydro-*N*-methyl-1-naphthalenamine hydrochloride (6.8 g, 0.02 mol) was suspended in NaOH aqueous solution (50 mL, 5 N) and ethyl acetate (50 mL) was gradually added. The mixture was stirred until two phases became clear. The organic phase was separated from the water phase and dried over Na_2SO_4 . The ethyl acetate was removed in vacuo and oily free base was obtained. Heptane (7 mL) was added and heated to 70 $^{\circ}\text{C}$. When cooled to room temperature, white crystals formed and were filtered off and dried at room temperature overnight in vacuo to give sertraline free base 4.9 g (yield: 80%).

Melting point: 69.25–69.87 $^{\circ}\text{C}$ (onset of DSC). ^1H NMR (DMSO- d_6 /TMS), δ (ppm): 1.67–1.72 (m, H), 1.87–1.94 (m, 2H), 1.96 (s, 1H), 2.00–2.06 (m, H), 2.35 (s, 3H), 3.61 (d, 1H), 4.08

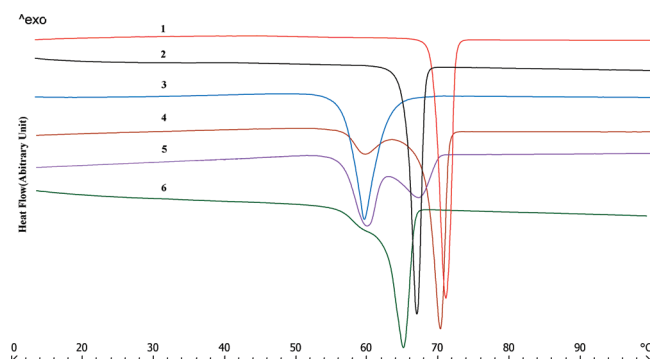


Figure 7. Representative DSC curves of mixtures with different enantiomeric compositions. 1, racemate; 2, enantiomer; 3, 4, 5, 6, are mixtures with $X_{1*S*,4*S*} = 0.85, 0.55, 0.65, 0.98$, respectively.

Table 2. Experimental Thermal Properties of Sertraline Racemate and Enantiomer

	sertraline racemate	sertraline enantiomer
melting point ($^{\circ}\text{C}$) (onset)	69.5 ± 0.5	66.5 ± 0.5
enthalpy of fusion (J/g)	70.0 ± 1.0	80.0 ± 1.0

(t, 1H), 6.69 (d, 1H), 7.08 (t, 1H), 7.14–7.17 (m, 2H), 7.375 (d, 1H), 7.405 (d, 1H), 7.545 (d, 1H). IR $\nu(\text{cm}^{-1})$: 2937(w), 2846(w), 2778(w), 1735(s), 1469(s), 1363(s), 1214(s), 1126(s), 1027(s).

2.3. Establishment of Binary Melting Point Phase Diagram. The mixtures with different enantiomeric compositions were prepared by mixing a weighed sertraline racemate (*cis*-sertraline) and enantiomer (*1S,4S*-sertraline). The resolution of balance was 0.00001 g. Differential scanning calorimetry (DSC) and spectroscopic analyses were performed on different parts of the sample and gave consistent results which confirmed sufficient mixing. The binary melting point phase diagram was established using Mettler Toledo DSC 822^o differential scanning calorimeter (Greifensee, Switzerland) by measuring the temperature at the beginning and the end of fusion of enantiomeric mixture. The samples (3–12 mg) were prepared in a

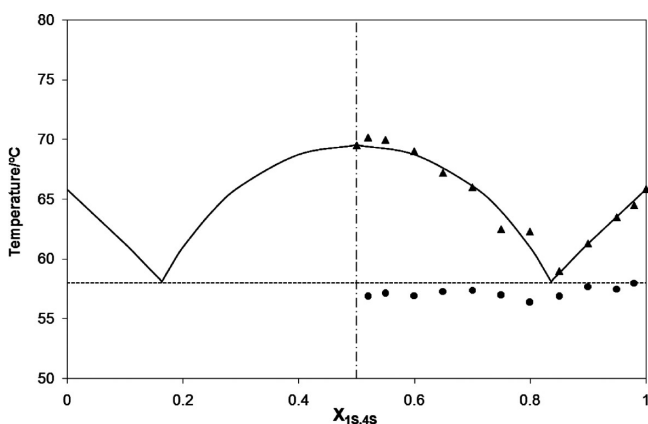


Figure 8. Binary melting point phase diagram of sertraline. The solid curves represent calculated liquidus lines; circle and triangle represent the temperatures of the beginning and the end of fusion respectively.

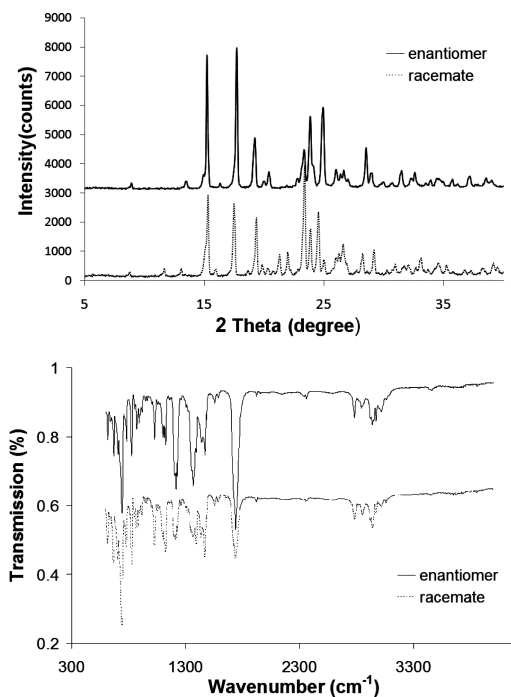


Figure 9. XRPD patterns (top) and FTIR spectra (bottom) of the racemate (lower traces) and enantiomer (upper traces).

covered aluminum crucible having pierced lids to allow the escape of volatiles. The sensors and samples were under nitrogen purge during the experiments. The temperature calibration was carried out using the melting point of highly pure indium in a medium temperature range. Heating rates of 3, 5, 10 °C/min were used. The heating rate did not affect the results. The heating rate of 5 °C/min was employed.

2.4. Single Crystal Preparation and Structure Determination. Sertraline racemate single crystals were grown from a concentrated ethanol solution by slow evaporation at room temperature. The translucent light colorless chip-like crystal was mounted on a glass fiber and data were collected at low temperature -150 K on a Nonius kappa-CCD area detector diffractometer with COLLECT using monochromatic Mo-K α radiation ($\lambda = 0.71073$ Å). Sertraline enantiomer single crystals were grown from a concentrated ethanol solution by slow evaporation at room temperature. The data were collected at temperature of 295 K on a 2D detector (Bruker Smart 6000 CCD) and 3-circle diffractometer (Bruker D8) using Cu-K α radiation ($\lambda = 1.54184$ Å). The structures were solved with direct method using the SHELXS-97 program and refined on F^2 's by full-matrix least-squares with the SHELXS-97 program. The calculated XRPD patterns based on single crystal data are in agreement with measured XRPD patterns. The comparisons are presented in the Supporting Information.

3. Results and Discussion

3.1. Solid Form of Sertraline Enantiomer. As described in Experimental Section, the solid sertraline enantiomer free base (*1S,4S*-sertraline) was isolated from its hydrochloride salt. Free base exists preferably in supercooled liquid form. Its solid form can crystallize from nonpolar solvent such as hexane, heptane, and toluene. In the thermograms of sertraline enantiomer, a single melting endothermic peak at 66.5 ± 0.5 °C (onset) was observed. Above 70 °C, there was no other obvious thermal event in the DSC trace until in the range of 250–360 °C, at which, another broad endothermic peak indicated the decomposition accompanying the almost complete weight loss in the thermogravimetric analysis (TGA) trace as shown in Figure 1. The heat of fusion, calculated by integration of the melting endotherm in the total heat flow,

Table 4. Crystal Structure Data of Sertraline Racemate and Enantiomer

	<i>cis</i> -sertraline	(<i>1S,4S</i>)-sertraline
empirical formula	C ₁₇ H ₁₇ Cl ₂ N	C ₁₇ H ₁₇ Cl ₂ N
formula weight (g/mol)	306.22	306.22
temperature (K)	150	295
wavelength(Å)	0.71073	1.54178
crystal system	monoclinic	monoclinic
space group	<i>P</i> 2 ₁ / <i>n</i> 1	<i>P</i> 2 ₁
<i>a</i> (Å)	11.0604(10)	8.7569(5)
<i>b</i> (Å)	8.6714(8)	8.7731(5)
<i>c</i> (Å)	16.2287(15)	10.7921(6)
α (°)	90	90
β (°)	103.937(6)	110.814(4)
γ (°)	90	90
<i>V</i> (Å ³)	1510.7(2)	775.00(8)
<i>D</i> _{calc} (g/cm ³)	1.346	1.312
<i>Z</i>	4	2
crystal size (mm)	0.06 × 0.08 × 0.2	0.4 × 0.4 × 0.4
reflections collected	10167	4996
goodness-of-fit on F^2	1.017	1.053
final <i>R</i> indices ($I > 2\sigma(I)$)	$R_1 = 0.0332$ $wR_2 = 0.0762$	$R_1 = 0.0347$ $wR_2 = 0.0981$
<i>R</i> indices (all data)	$R_1 = 0.0469$ $wR_2 = 0.0827$	$R_1 = 0.0354$ $wR_2 = 0.0993$

Table 3. XRPD Peaks of Sertraline Racemate and Enantiomer

	$2\theta/^\circ$												
enantiomer	15.20	17.65	19.15	20.31	23.25	23.81	24.85	25.90	28.41	28.90	31.31	32.45	
racemate	13.12	15.23	17.42	19.25	21.28	21.89	23.30	23.84	24.49	26.48	28.13	29.00	32.99

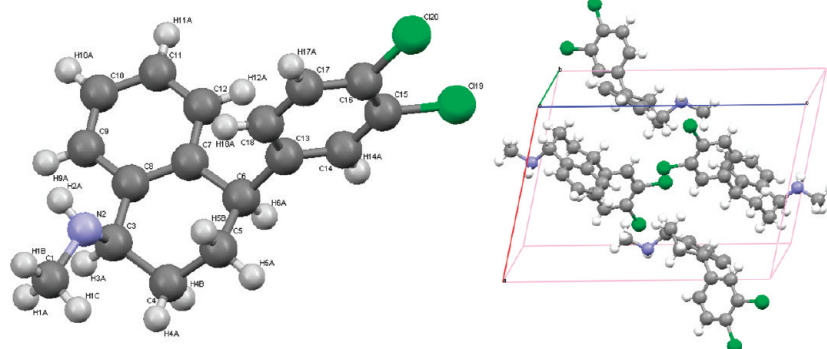


Figure 10. Atomic-numbering molecule scheme (left) and four molecules in the unit cell (right) of sertraline racemate.

was 70.0 ± 1.0 J/g. Further hot stage microscope (HSM) investigation confirmed the interpretation of thermal events happened when the crystalline free base experienced the heating process in the DSC crucible. The photomicrographs are displayed in Figure 2. Figure 2a shows the powder samples of sertraline at 25 °C. When heated to 65 °C, a small move of crystals was observed. At 67 °C shown in Figure 2b, the crystals started to melt and the edge became round, then quickly the crystals melted completely to form bigger liquid droplets at 71 °C shown in Figure 2c,d.

The polymorphic outcome of crystallization is usually system-specific, and it could be influenced by a number of factors such as temperature, solvent, supersaturation, cooling rate, agitation rate, impurity, and additives.²⁰ The mechanism of these effects is not well-known, and the quantitative relationship between the operational factors and the polymorphic outcome is not clearly understood.²¹ Exploring new crystal forms relies basically on traditional experimental methods. Since most APIs are purified and isolated by crystallization from an appropriate solvent, the most prevalent method of polymorph screening starts with crystallization of APIs from a number of solvents.^{9,22} The solvents used in this study included ethanol, methanol, 2-propanol, and mixtures of hexane and alcohol. All the resulting solids showed the same melting point and XRPD patterns as those of the original sertraline enantiomer free base crystals. The sertraline free base was further suspended in the above-mentioned organic solvents and water under vortex for 48 h. There was no evidence indicating the existence of solvate or hydrate by analyzing the solid phases at equilibrium. This result is further supported by the latter crystal structure investigation work in which all concerned single crystals grown from different solvents showed the same unit cell and the theoretical calculated X-ray patterns of single crystal were completely coincident with the powder X-ray patterns of bulk samples.

Heat-cool-heat cycles and crystallization from melt are efficient ways to detect new polymorphs. So the crystalline sertraline enantiomer was subjected to a heat-cool-heat cycle in DSC measurements shown in Figure 3a, namely, heating from 20 to 120 °C at 5 °C/min, then cooling from 120 to 20 °C at 10 °C/min, and reheating from 20 to 120 °C at 5 °C/min. The DSC curve from the first heating segment 1 showed one sharp endotherm peak and matched the melting behavior of sertraline enantiomer. There were no obvious sharp exothermic peaks in the DSC curve when samples in the DSC crucible underwent the cooling process (segment 2) and then immediately the reheating process (segment 4); there were no obvious sharp endotherm peaks in the DSC

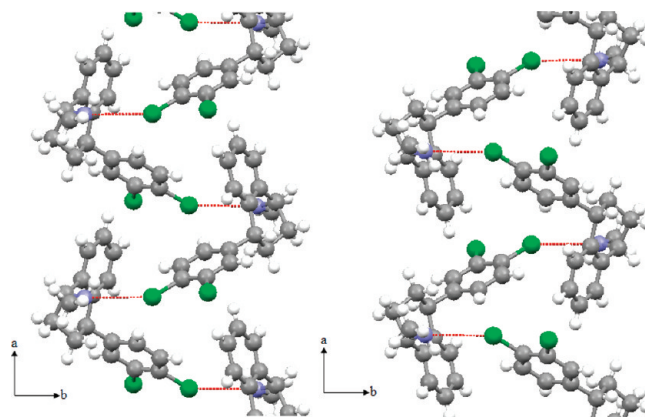


Figure 11. H-bond patterns of (1R,4R) (left) and (1S,4S) (right) columns in the racemate.

curve from the reheating run. Small thermal events happened during segments 2 and 4 marked in red circles. The DSC curve indicated that the melt did not crystallize immediately and completely during the cooling process. Since the supercooling is a necessary condition for crystallization and the degree of supercooling depends on the nature of substance and is influenced by the heat transfer as well as the cooling rate,²³ the sertraline enantiomer melts after the first heating process were subjected to different cooling rates, namely, 0.1, 1, 5, and 10 °C/min, respectively, in expectation to provide enough time to reach thermal equilibrium and let the molecule relax, nucleate, and grow. The DSC traces under these cooling rates did not change much and were still similar to that in Figure 3a.

However, the sample in the crucible after the first melting process was taken out from the DSC and left at room temperature overnight, then was run on DSC and XRPD again. The DSC curve of the second heating run displayed the same endotherm peak as first heating run; just the onset of melting point and heat of fusion decreased a little bit probably due to the presence of a small amount of liquid remaining or degradation of the sample. The XRPD pattern was consistent with that of the original sertraline enantiomer. Both XRPD and DSC results implied that the solid crystallized from melt at room temperature was same as the original form of sertraline enantiomer. The assumption was verified by extending the annealing time of sample in the DSC crucibles at room temperature. The samples staying at room temperature more than one week after the first heating and melting process exhibited almost the same melting point and heat of fusion as the original sertraline enantiomer.

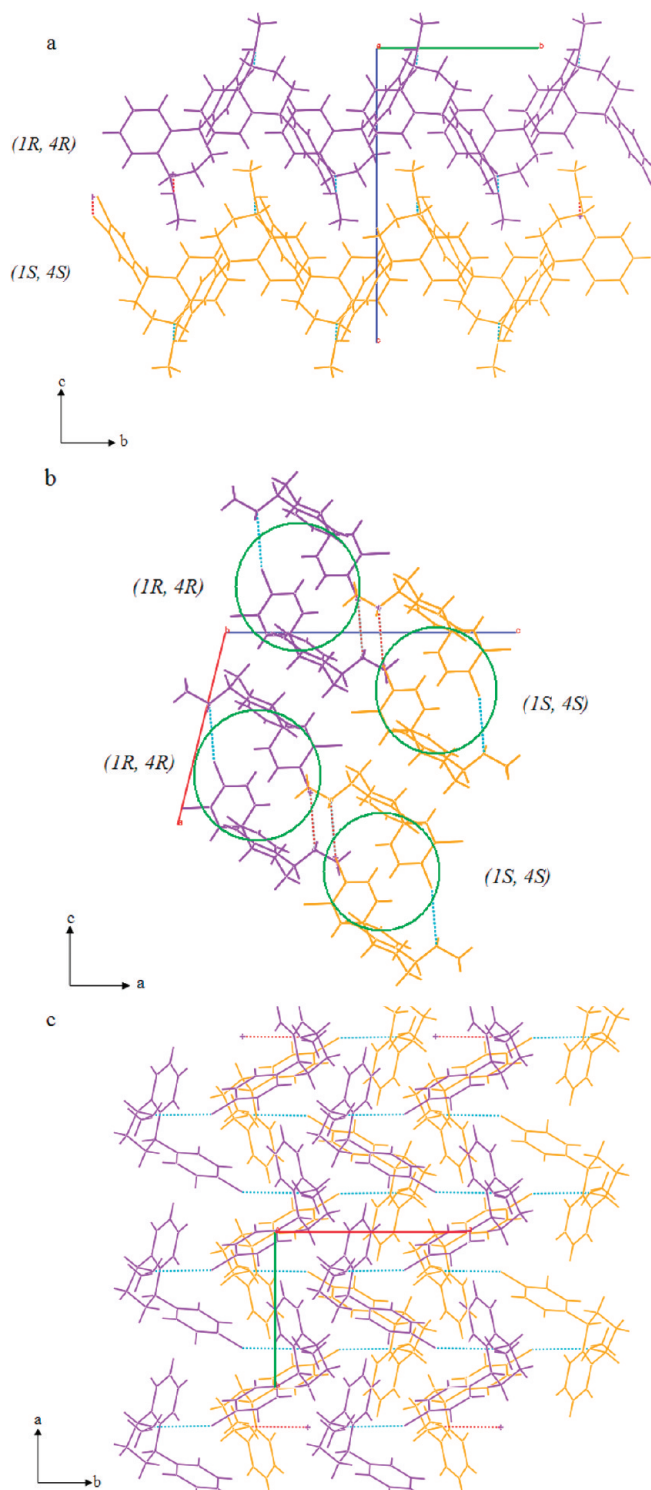


Figure 12. Crystal packing diagram of the racemate. Purple and orange represent (1*R*,4*R*) and (1*S*,4*S*) molecules, respectively; dotted blue and red lines represent hydrogen bonds.

In order to further track the crystallization during the cooling and annealing process, the sample in the DSC crucible after the first heating run segment 1 was cooled down to 20 °C (segment 2), kept at that temperature for 10 h under inert N₂ atmosphere (segment 3), and then experienced the second heating run in segment 4, in which the heating and cooling rates were exactly same as that in Figure 3a. The recorded DSC trace is depicted in Figure 3b.

During the cooling process, a small endotherm peak and then an exotherm peak (in red circles) were observed, which might result from phase transition or crystallization. During the annealing process at 20 °C, several flat exotherm peaks (in red circles) were seen in the first 140 min as shown in Figure 3b of segment 3. They might be crystallization, crystal growth, or phase transformation. The very flat line appeared in the last 460 min shown in segment 3 implied no other thermal events happened. Upon the second heating, only one sharp endotherm peak (segment 4) was observed that corresponded to the same melting behavior of starting sertraline enantiomer. These results are in agreement with the crystal annealed at room temperature under air atmosphere.

The crystallization from melt was also tracked in situ by recording XRPD patterns profile as a function of time at room temperature. The sertraline free base was heated and melted on the XRPD sampler directly, and then the XRPD patterns were recorded continuously. As shown in Figure 4, the starting melt did not exhibit any peaks, and after 30 min there emerged some peaks showing the occurrence of crystallization. More and more sertraline enantiomer-related peaks appeared and their intensity increased. After 2–3 h, all the characteristic peaks appeared. These peaks could be ascribed to the sertraline enantiomer. However, even after 96 h, the diffraction peak intensities were still lower than those in the original sertraline enantiomer, which may be caused by a small amount of melt, disordered component, or amorphous phase in the resulting solid. Besides the characteristic peaks of original sertraline enantiomer solid, there were no other detectable peaks. Therefore, no obvious phase transformation was observed. Although we cannot completely exclude the possibility of existence of other metastable phases as well as phase transition during the melt crystallization process, the XRPD patterns shown in Figure 4 confirmed that the final solid crystallized from melt was the same as the original form of sertraline enantiomer.

Observations from HSM provided further support to our conclusion. When the melting liquid under the HSM was cooled and annealed at room temperature, the sample did not crystallize immediately. Only part of liquid transformed into crystals as shown in Figure 5a. Part of the melt samples on the slide under HSM still existed as small liquid droplets even after one week. The newly crystallized solid from melt was reheated in hot stage, and the snapshots of melting behavior were recorded. At 65 °C, the crystals started to blur and turned into transparent liquid as shown in Figure 5b–d upon melting.

In light of DSC, XRPD, and HSM investigations, the melt sertraline enantiomer cannot crystallize immediately and requires enough annealing time at room temperature to crystallize as the original form. The crystallization is a very complicated process especially in polymorphic systems, which may involve nucleation, crystal growth, the competition between polymorphs as well as the effects of supercooling degree and impurity, etc.^{23,24} According to Ostwald's rule,²⁵ the metastable polymorph preferably crystallizes first and then converts to the more stable form. So the above observed crystallization phenomenon might result from the combination of nucleation kinetics and growth kinetics. These endo/exo thermal events in segments 2, 3, and 4 in Figure 3a,b are most likely the results of metastable phase nucleation and growth, metastable phase transformation into stable phase as well as stable phase crystallization,

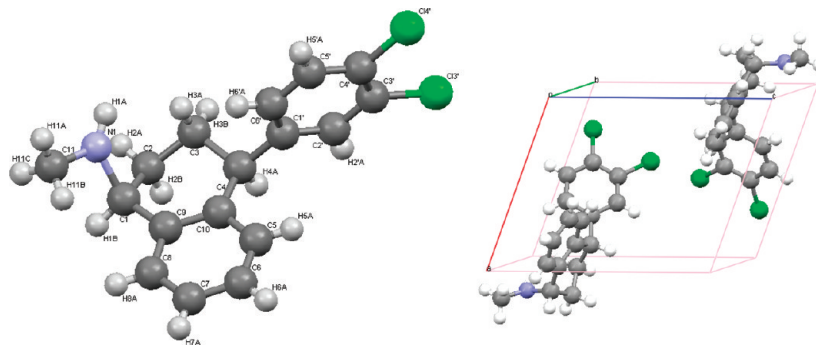


Figure 13. Atomic-numbering enantiomer molecule scheme (left) and two molecules in the unit cell (right) of sertraline enantiomer.

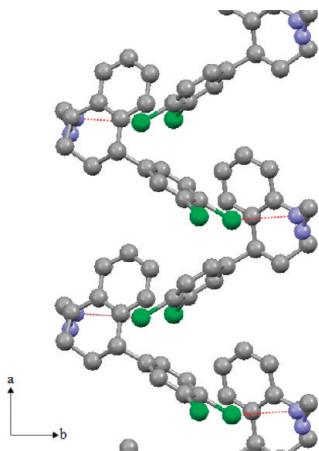


Figure 14. H-bond pattern of $(1S,4S)$ column in the enantiomer.

etc. Although we cannot verify crystallization and transformation kinetics clearly, the final obtained form from the melt is undoubtedly the same polymorphic form as the original sertraline enantiomer.

The above polymorph screening investigation provides no evidence of other stable polymorphs and solvates of sertraline enantiomer. Since the number of polymorphs of a given compound is proportional to the time and money spent on the compound,²⁶ we cannot prove definitively that the sertraline enantiomer has no polymorphic distribution. However, under our current investigation, at least we believe that it was not easy to generate other forms, especially solvate forms. The obtained crystalline form was quite stable at room temperature. Interestingly, the preliminary inference coincided with the phenomenon observed in another antidepressant drug, venlafaxine, which demonstrated no polymorphism of the free base compared to the venlafaxine hydrochloride.²⁷

3.2. Properties of Solid-State Sertraline Enantiomer. Solubility of API in water and/or organic solvents is a key physical parameter for compatibility with various dosage forms. The solubility of sertraline enantiomer free base in water was measured by gravimetric method. The starting solid was suspended in water for 24, 48, 72, and 96 h, respectively. Experimental results indicate that 72 h is sufficient to reach dissolution equilibrium. The undissolved solid phase at equilibrium was analyzed by XRPD, Raman, and DSC. All the characterization methods confirmed that the final form was identical to the starting solid phase. The comparison of XPRD patterns belonging to the starting solid and the undissolved solid in solubility experiments is

provided in Supporting Information. The pH value of saturated solution at equilibrium was measured using a pH meter. The solubilities of sertraline free base and its salts are summarized in Table 1.

Hygroscopicity is another important physical property of the API for formulation. The hygroscopicity of sertraline enantiomer free base and sertraline hydrochloride was measured by dynamic vapor sorption (DVS). The relative humidity (RH) ranged from 0% to 90%, with steps of 10%. Both sertraline free base and its hydrochloride salt have very low hygroscopicity as is shown in Figure 6. The equal mass increase and decrease in a DVS measurement cycle also allude to the nonexistence of sertraline hydrate, which is consistent with the observation from solvate screening in Section 3.1.

On the basis of the above investigation, crystalline sertraline enantiomer has hygroscopicity similar to sertraline hydrochloride but exhibits much less polymorphic diversity, which provides an advantage for a potential alternative API formulation. Although the solubility of sertraline base is very low, the drawback can be overcome with proper formulation strategies such as nanosizing, adding a solubility enhancer and using novel drug delivery systems including micelle, micro-emulsion or emulsion, solid lipid nanoparticles, etc.^{28–30}

3.3. Binary Phase Diagram of Sertraline. The solid sertraline racemate was also obtained as described in Experimental Section and its solid nature was investigated. The thermal analysis of mixtures of sertraline racemate (*cis*-sertraline) and sertraline enantiomer ($(1S,4S)$ -sertraline) by DSC was studied in the range of 0.5–1.0 molar fraction of sertraline enantiomer.

The preparation of mixtures with different enantiomeric compositions was conducted in three different ways to eliminate the influence of sample preparation method. First, a weighed amount of sertraline enantiomer was physically mixed with sertraline racemate and crushed in a mortar and pestle to obtain a uniform mixture. Second, a weighed mixture was dissolved in methanol to ensure uniform mixing and then the solvent was evaporated. Third, a weighted mixture was melted and then solidified. Namely, the samples obtained by mortar and pestle mixing were run on DSC, annealed one day in a crucible, and then run on DSC for a second time. All three methods gave consistent DSC curves and demonstrated that the physical mixing method to prepare samples by mortar and pestle was feasible. In this work, mixtures with different enantiomeric compositions were prepared by a physical mixing method. The interesting point was that even the mixtures obtained by melting did not give a different DSC curve, which suggested that no

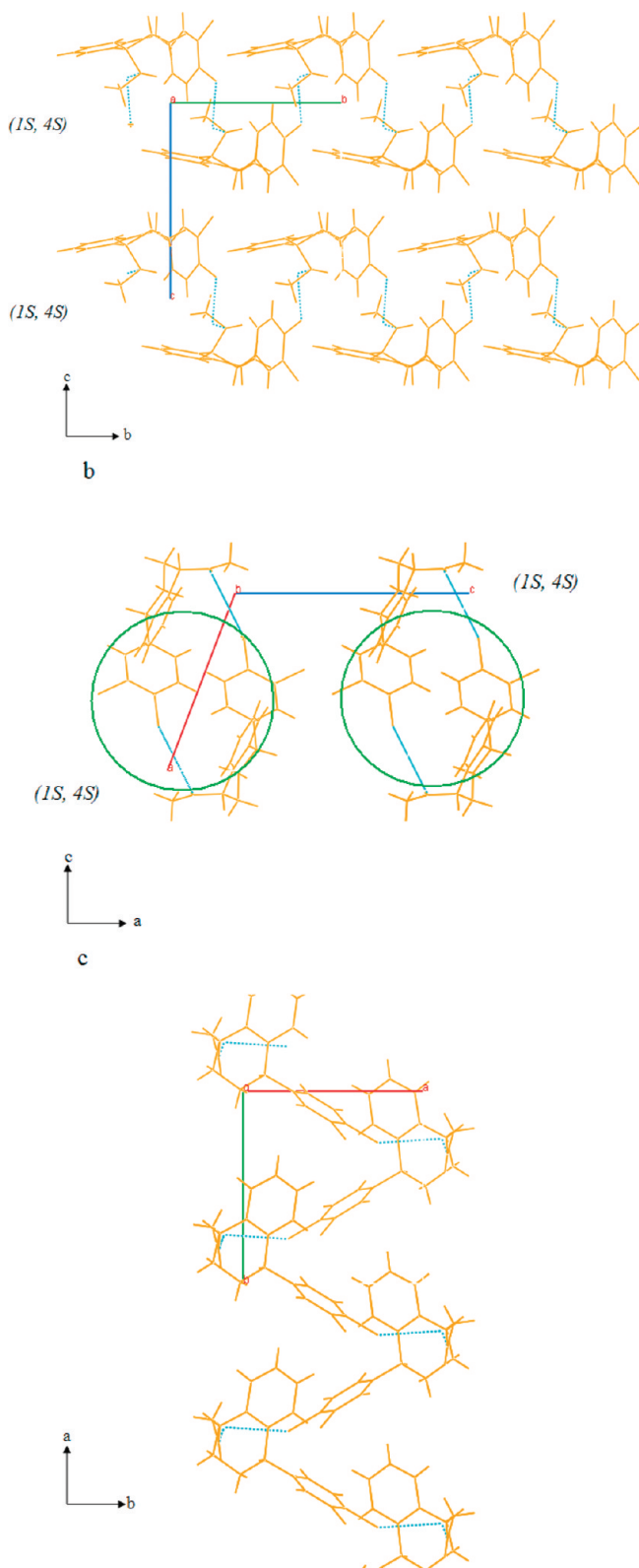


Figure 15. Crystal packing diagram of the enantiomer. Dotted blue lines represent hydrogen bonds and the disorder of the methylamine group is not shown for clarity.

other phases formed from the melt crystallization. This implies less polymorphic potency of sertraline enantiomer and racemate.

The DSC curves of pure racemate and enantiomer exhibited one sharp endothermic peak represented by curves 1

and 2, respectively, as shown in Figure 7. The thermal data are listed in Table 2.

Other mixtures with different enantiomeric compositions had two distinct peaks as curves 3, 4, 5, 6, and 7 shown in Figure 7. The first endothermic peak represented the fusion of the eutectic. The solidus temperature (T_e) was determined by the onset temperature of the first peak. The second peak, however, represented the melting effect of the excess (*1S,4S*)-enantiomer in the melting process. The liquidus temperature (T_f) was determined by peak temperature of the second peak. Curve 3 denotes the mixture with molar fraction of 0.85 as an exception. It exhibited only one melting peak with the onset temperature of 56.85 °C. The first peaks' melting temperature of all other mixtures coincided with 56.85 ± 1 °C, which implies that the eutectic point is located at $X_{1S,4S} = 0.85$ with a melting point of 56.85 °C.

The DSC curves present a typical racemic compound feature. However, it is well-known that the partial solid solution may exist in certain enantiomeric composition regions. Partial solid solution happens most often in the vicinity of racemate and/or enantiomer¹² and less often in the other regions.³¹ The mixture with $X_{1S,4S} = 0.98$ still displays a notable melting event at the eutectic melting temperature and rules out the possibility of solid solution. As for $X_{1S,4S}$ from 0.98 to 1.0, we cannot provide a reasonable explanation if there is a partial solid solution in the narrow vicinity of enantiomer. Usually, a Tammann-plot using the heat of fusion of eutectic vs enantiomeric composition can rule out the possibility of solid solution in the vicinity of pure enantiomer.¹² However, in this case, the Tammann-plot was not feasible in that the melting temperature of 56.85 °C and enantiomeric composition of 0.84 of eutectic were fairly near to those of enantiomer and the merging of two melting peaks in DSC curves made it difficult to determine the heat of fusion by integrating areas of peaks accurately.

The resulting binary diagram is depicted in Figure 8 for the mole fraction of (*1S,4S*)-sertraline $X_{1S,4S}$ ranging from 0.5 to 1. The experimental values agree well with the two theoretical liquidus curves (the solid curves in Figure 8) assuming the system is a racemic compound. The two theoretical liquidus curves were calculated respectively on the basis of the melting point and fusion enthalpy of sertraline enantiomer using Schroder-van Laar equation,

$$\ln X_R = \frac{\Delta H_{R,f}}{R} \left(\frac{1}{T_{R,f}} - \frac{1}{T_f} \right),$$

and the melting point and fusion enthalpy of *cis*-sertraline racemate using Prigogine-Defay equation,

$$\ln 4X_R(1-X_R) = \frac{2\Delta H_{rac,f}}{R} \left(\frac{1}{T_{rac,f}} - \frac{1}{T_f} \right),$$

where X_R is the molar fraction of enantiomer, $\Delta H_{R,f}$ and $T_{R,f}$ are the enthalpy of fusion in J/mol and the melting point of pure enantiomer in K, $\Delta H_{rac,f}$ and $T_{rac,f}$ are the enthalpy of fusion of racemate in J/mol and the melting point of racemate in K, and R is a gas constant.¹²

The two theoretically calculated curves intersect at $X_{1S,4S} = 0.84$ and $T_e = 58$ °C, which is in good agreement with the experimental values of $X_{1S,4S} = 0.85$ and $T_e = 56.85$ °C. Therefore, the sertraline system is determined as a racemic compound.

Table 5. Bond Lengths, Bond Angles for Sertraline Racemate

Bond Lengths (Å)			
C1–N2	1.454	C8–C9	1.406
C1–H1A	0.98	C9–C10	1.386
C1–H1B	0.98	C9–H9A	0.95
C1–H1C	0.98	C10–C11	1.381
N2–C3	1.47	C10–H10A	0.95
N2–H2A	0.85	C11–C12	1.380
C3–C8	1.513	C11–H11A	0.95
C3–C4	1.53	C12–H12A	0.95
C3–H3A	1.0	C13–C14	1.388
C4–C5	1.525	C13–C18	1.397
C4–H4A	0.99	C14–C15	1.395
C4–H4B	0.99	C14–H14A	0.95
C5–C6	1.535	C15–C16	1.394
C5–H5A	0.99	C15–C119	1.738
C5–H5B	0.99	C16–C17	1.385
C6–C7	1.534	C16–C120	1.740
C6–H6A	1.0	C17–C18	1.379
C6–C13	1.52	C17–H17A	0.95
C7–C12	1.398	C18–H18A	0.95
C7–C8	1.400		
Bond Angles (°)			
N2–C1–H1A	109.5	C12–C7–C6	119.21(17)
N2–C1–H1B	109.5	C8–C7–C6	121.90(17)
N2–C1–H1C	109.5	C7–C8–C9	118.62(18)
H1A–C1–H1B	109.5	C7–C8–C3	122.31(17)
H1A–C1–H1C	109.5	C9–C8–C3	119.06(18)
H1B–C1–H1C	109.5	C10–C9–C8	121.5(2)
C1–N2–C3	113.82(17)	C10–C9–H9A	119.2
C1–N2–H2A	106.6(16)	C8–C9–H9A	119.2
C3–N2–H2A	109.3(16)	C11–C10–C9	119.5(2)
N2–C3–C8	108.22(16)	C11–C10–H10A	120.3
N2–C3–C4	110.74(17)	C9–C10–H10A	120.3
N2–C3–H3A	108.8	C12–C11–C10	119.8(2)
C8–C3–C4	111.34(16)	C12–C11–H11A	120.1
C8–C3–H3A	108.8	C10–C11–H11A	120.1
C4–C3–H3A	108.8	C11–C12–C7	121.7(2)
C5–C4–C3	110.53(16)	C11–C12–H12A	119.1
C5–C4–H4A	109.5	C7–C12–H12A	119.1
C5–C4–H4B	109.5	C14–C13–C18	118.16(17)
C3–C4–H4A	109.5	C14–C13–C6	120.93(16)
C3–C4–H4B	109.5	C18–C13–C6	120.90(17)
H4A–C4–H4B	108.1	C13–C14–C15	120.64(17)
C4–C5–C6	110.38(17)	C13–C14–H14A	119.7
C4–C5–H5A	109.6	C15–C14–H14A	119.7
C4–C5–H5B	109.6	C16–C15–C14	120.34(17)
C6–C5–H5A	109.6	C16–C15–C119	120.46(15)
C6–C5–H5B	109.6	C14–C15–C119	119.20(14)
H5A–C5–H5B	108.1	C15–C16–C17	119.39(18)
C13–C6–C7	111.31(15)	C15–C16–C120	121.43(15)
C13–C6–C7	111.31(15)	C17–C16–C120	119.19(15)
C13–C6–C5	111.57(15)	C18–C17–C16	120.17(18)
C13–C6–H6A	107.1	C18–C17–H17A	119.9
C7–C6–C5	112.24(16)	C16–C17–H17A	119.9
C7–C6–H6A	107.1	C17–C18–C13	121.29(18)
C5–C6–H6A	107.1	C17–C18–H18A	119.4
C12–C7–C8	118.88(18)	C13–C18–H18A	119.4
Torsion Angles (°)			
C1–N2–C3–C8	163.01(18)	C9–C10–C11–C12	−0.4(3)
C1–N2–C3–C4	−74.7(2)	C10–C11–C12–C7	−0.4(3)
N2–C3–C4–C5	−70.0(2)	C8–C7–C12–C11	0.9(3)
C8–C3–C4–C5	50.5(2)	C6–C7–C12–C11	179.63(18)
C3–C4–C5–C6	−64.9(2)	C7–C6–C13–C14	−115.5(2)
C4–C5–C6–C13	170.76(16)	C5–C6–C13–C14	118.3(2)
C4–C5–C6–C7	45.0(2)	C7–C6–C13–C18	64.2(2)
C13–C6–C7–C12	41.0(2)	C5–C6–C13–C18	−62.0(2)
C5–C6–C7–C12	166.85(17)	C18–C13–C14–C15	0.6(3)
C13–C6–C7–C8	−140.31(18)	C6–C13–C14–C15	−179.64(16)
C5–C6–C7–C8	−14.4(2)	C13–C14–C15–C16	0.6(3)
C12–C7–C8–C9	−0.5(3)	C13–C14–C15–C119	−179.45(14)
C6–C7–C8–C9	−179.17(17)	C14–C15–C16–C17	−0.8(3)

Table 5. Continued

Torsion Angles (°)			
C12–C7–C8–C3	–179.65(17)	C119–C15–C16–C17	179.20(14)
C6–C7–C8–C3	1.6(3)	C14–C15–C16–C120	179.20(14)
N2–C3–C8–C7	102.3(2)	C119–C15–C16–C120	–0.8(2)
C4–C3–C8–C7	–19.6(2)	C15–C16–C17–C18	–0.2(3)
N2–C3–C8–C9	–76.9(2)	C120–C16–C17–C18	179.83(15)
C4–C3–C8–C9	161.20(17)	C16–C17–C18–C13	1.4(3)
C7–C8–C9–C10	–0.4(3)	C14–C13–C18–C17	–1.6(3)
C3–C8–C9–C10	178.82(17)	C6–C13–C18–C17	178.66(18)
C8–C9–C10–C11	0.9(3)		

In addition, the comparison of the structural difference between enantiomers and racemates by spectra analysis such as FTIR, Raman, or SSNMR and XRPD patterns of racemate and enantiomer further confirms the racemate solid nature. It is generally accepted that identical spectra and XRPD patterns suggest a conglomerate, similar spectra and XRPD patterns imply a pseudoracemate and different spectra and XRPD patterns represent a racemic compound.

The XRPD pattern of sertraline racemate was different from that of the corresponding enantiomer shown in Figure 9 (top). The racemate compound had peaks at the following 2θ angles: 8.79°, 15.23°, 17.42°, 19.25°, 21.28°, 21.89°, 23.30°, 23.84°, 24.49°, 26.48°, 28.13°, 29.09°, 32.99°, whereas the enantiomer had peaks at 8.89°, 13.46°, 15.20°, 17.65°, 19.15°, 20.31°, 23.25°, 23.81°, 24.85°, 25.90°, and 28.41°, 28.90°, 31.31°, 32.45°. They have some similar peaks; however, the enantiomer has unique peaks at 13.46°, 20.31°, 25.90°, 31.31°, 32.45° and the racemate has unique peaks at 13.12°, 21.28°, 21.89°, 26.48°, and 32.99°. These values are tabulated in Table 3 for clarity.

Figure 9 (bottom) exemplifies the FTIR spectra of sertraline racemate and enantiomer. FTIR of the racemate is almost superimposable on that of enantiomer and the most notable difference is at wavenumber 1365–1394 cm^{-1} and 3450 cm^{-1} .

These FTIR spectroscopic analyses and XPRD patterns provide further support of the racemic compound nature of sertraline racemate free base.

3.4. Molecular and Crystal Structure of Sertraline. The crystal structures of both sertraline racemate and enantiomer were obtained through X-ray crystallographic diffraction analysis. It was confirmed that sertraline racemate existed as a racemic compound. The structure was solved and refined successfully in $P12_1/n1$ space group with $Z = 4$, whereas the structure of the sertraline enantiomer belonged to $P2_1$ space group with $Z = 2$. Detailed crystal structure data are summarized in Table 4.

In the crystal of the racemate, two (*IR,4R*) and two (*IS,4S*) molecules are paired and packed in crystal unit cell to form the racemate as shown in Figure 10 (right). All molecules have the same conformation. The atomic-numbering molecule is shown in Figure 10 (left). The molecule skeleton basically includes a head formed by the methylamine group, a central part composed by a phenyl and cyclohexane ring from C6–C12, and a tail part of a chlorine-substituted phenyl ring from C13–C120. Except for a small deviation of C4 and C5, the central phenyl ring and cyclohexane ring are in one plane. The C1, N2, and C3 are in another plane, making an angle of 82.63° with the central plane. The tail part aromatic ring define another plane which is almost vertical to the central plane with an inter planar

angle of 84.19°. The hydrogen-bonding plays a key role in determining the crystal packing. Surprisingly, there are no hydrogen-bonding interactions between the heterochiral (*IR,4R*) molecule and (*IS,4S*) molecule, whereas there are hydrogen-bonding interactions between homochiral molecules. As shown in Figure 11 (left), (*IR,4R*) molecules are linked to each other head to tail by hydrogen bonds, namely, a head H of N to a tail Cl of another neighboring molecule, which form a catemer hydrogen-bonding motif. The hydrogen bond is relatively strong with N–Cl = 3.229 Å. The homochiral molecules are aligned and extended along the *b*-axis to form an infinite hollow column viewed from the *b*-axis. (*IS,4S*) molecules are orientated head to tail by hydrogen bond in the same manner displayed in Figure 11 (right), and thus another homochiral column along the *b*-axis is also obtained. These (*IR,4R*) and (*IS,4S*) columns are parallel one to another and are assembled alternatively to form a compact crystal structure favorable to the stability of the racemate. The packing diagrams are illustrated in Figure 12 viewed from the *a*, *b*, and *c*-axis, respectively.

In the crystal of enantiomer, two (*IS,4S*) molecules exist in the unit cell in Figure 13 (right). The atomic-numbering molecule is shown in Figure 13 (left). The molecule skeleton has almost the same shape as the racemate molecule including the methylamine group as a head part, the phenyl and hexane ring as a central part and a tail part of chlorine-substituted phenyl ring. The phenyl rings and cyclohexane ring are in a well-defined arrangement. The two aromatic planes in one molecule make an angle of 83.33°, which is slightly different from that in the racemate. However, there are some disorders in the methylamine head part in the molecule. This part can adopt two orientations relative to the central phenyl ring and cyclohexane ring, differing from each other in the N1 position. The atomic coordinates of N1 in conformation 1 and N1A in conformation 2 are (–0.1365, –0.1738, 0.8492) Å and (–0.1058, 0.2536, 0.8708) Å, respectively. The head part C11, N1, and C1 in conformation 1 forms a plane making angle of 59.28° with the central part aromatic ring plane, which are significantly different from that of 82.63° in the racemate, whereas the C11A, N1A, and C1A plane in conformation 2 makes an angle of 80.42° with the central part aromatic ring plane, which are slightly different from that of 82.63° in the racemate. (*IS,4S*) molecules are also oriented head to tail and linked by hydrogen bonds, between a head H of N to a tail Cl of another neighboring molecule as illustrated in Figure 14. The distance of N–Cl is 3.274 Å. (*IS,4S*) molecules are aligned along the *b*-axis to form an infinite hollow column in the same way as the racemate. Thus, two columns are parallel to one another and stack to form homochiral crystals. The packing diagram is clearly shown in Figure 15.

Table 6. Bond Lengths, Bond Angles for Sertraline Enantiomer

Bond Lengths / Å			
C(1)–C(9)	1.489(4)	C(4)–H(4A)	0.9800
C(1)–C(2)	1.515(5)	C(5)–C(6)	1.372(4)
C(1)–N(1)	1.535(10)	C(5)–C(10)	1.392(3)
C(1)–H(1B)	0.9800	C(5)–H(5A)	0.9300
N(1)–C(11)	1.449(14)	C(6)–C(7)	1.341(5)
N(1)–H(1A)	0.8600	C(6)–H(6A)	0.9300
C(11)–H(11A)	0.9600	C(7)–C(8)	1.366(5)
C(11)–H(11B)	0.9600	C(7)–H(7A)	0.9300
C(11)–H(11C)	0.9600	C(8)–C(9)	1.430(4)
N(1A)–C(11A)	1.440(5)	C(8)–H(8A)	0.9300
N(1A)–H(1C)	0.8600	C(9)–C(10)	1.394(3)
C(11A)–H(11D)	0.9600	C(1')–C(2')	1.379(3)
C(11A)–H(11E)	0.9600	C(1')–C(6')	1.389(4)
C(11A)–H(11F)	0.9600	C(2')–C(3')	1.390(3)
C(2)–C(3)	1.530(4)	C(2')–H(2'A)	0.9300
C(2)–H(2A)	0.9700	C(3')–C(4')	1.384(3)
C(2)–H(2B)	0.9700	C(3')–Cl(3')	1.727(2)
C(3)–C(4)	1.530(4)	C(4')–C(5')	1.378(4)
C(3)–H(3A)	0.9700	C(4')–Cl(4')	1.730(2)
C(3)–H(3B)	0.9700	C(5')–C(6')	1.369(4)
C(4)–C(10)	1.521(3)	C(5')–H(5'A)	0.9300
C(4)–C(1')	1.523(3)	C(6')–H(6'A)	0.9300
Bond Angles / °			
C(9)–C(1)–C(2)	111.7(2)	C(1')–C(4)–H(4A)	107.0
C(9)–C(1)–N(1)	123.2(4)	C(3)–C(4)–H(4A)	107.0
C(2)–C(1)–N(1)	89.1(5)	C(6)–C(5)–C(10)	122.1(3)
C(9)–C(1)–H(1B)	110.3	C(6)–C(5)–H(5A)	118.9
C(2)–C(1)–H(1B)	110.3	C(10)–C(5)–H(5A)	118.9
N(1)–C(1)–H(1B)	110.3	C(7)–C(6)–C(5)	119.5(3)
C(11)–N(1)–C(1)	103.9(10)	C(7)–C(6)–H(6A)	120.2
C(11)–N(1)–H(1A)	128.1	C(5)–C(6)–H(6A)	120.2
C(1)–N(1)–H(1A)	128.1	C(6)–C(7)–C(8)	121.0(3)
N(1)–C(11)–H(11A)	109.5	C(6)–C(7)–H(7A)	119.5
N(1)–C(11)–H(11B)	109.5	C(8)–C(7)–H(7A)	119.5
H(11A)–C(11)–H(11B)	109.5	C(7)–C(8)–C(9)	121.3(3)
N(1)–C(11)–H(11C)	109.5	C(7)–C(8)–H(8A)	119.4
H(11A)–C(11)–H(11C)	109.5	C(9)–C(8)–H(8A)	119.4
H(11B)–C(11)–H(11C)	109.5	C(10)–C(9)–C(8)	117.0(3)
C(11A)–N(1A)–H(1C)	123.8	C(10)–C(9)–C(1)	122.4(2)
N(1A)–C(11A)–H(11D)	109.5	C(8)–C(9)–C(1)	120.6(3)
N(1A)–C(11A)–H(11E)	109.5	C(5)–C(10)–C(9)	119.1(2)
H(11D)–C(11A)–H(11E)	109.5	C(5)–C(10)–C(4)	119.0(2)
N(1A)–C(11A)–H(11F)	109.5	C(9)–C(10)–C(4)	121.8(2)
H(11D)–C(11A)–H(11F)	109.5	C(2')–C(1')–C(6')	118.1(2)
H(11E)–C(11A)–H(11F)	109.5	C(2')–C(1')–C(4)	120.9(2)
C(1)–C(2)–C(3)	110.5(3)	C(6')–C(1')–C(4)	121.0(2)
C(1)–C(2)–H(2A)	109.5	C(1')–C(2')–C(3')	120.9(2)
C(3)–C(2)–H(2A)	109.5	C(1')–C(2')–H(2'A)	119.6
C(1)–C(2)–H(2B)	109.5	C(3')–C(2')–H(2'A)	119.6
C(3)–C(2)–H(2B)	109.5	C(4')–C(3')–C(2')	120.0(2)
H(2A)–C(2)–H(2B)	108.1	C(4')–C(3')–Cl(3')	120.63(17)
C(2)–C(3)–C(4)	109.9(3)	C(2')–C(3')–Cl(3')	119.40(16)
C(2)–C(3)–H(3A)	109.7	C(5')–C(4')–C(3')	119.2(2)
C(4)–C(3)–H(3A)	109.7	C(5')–C(4')–Cl(4')	119.45(19)
C(2)–C(3)–H(3B)	109.7	C(3')–C(4')–Cl(4')	121.32(18)
C(4)–C(3)–H(3B)	109.7	C(6')–C(5')–C(4')	120.5(2)
H(3A)–C(3)–H(3B)	108.2	C(6')–C(5')–H(5'A)	119.8
C(1)–C(2)–C(3)	110.5(3)	C(4')–C(5')–H(5'A)	119.8
C(1)–C(2)–H(2A)	109.5	C(5')–C(6')–C(1')	121.3(2)
C(3)–C(2)–H(2A)	109.5	C(5')–C(6')–H(6'A)	119.4
C(1)–C(2)–H(2B)	109.5	C(1')–C(6')–H(6'A)	119.4
Torsion Angles / °			
C(9)–C(1)–N(1)–C(11)	–86.6(10)	C(1')–C(4)–C(10)–C(5)	–40.1(3)
C(2)–C(1)–N(1)–C(11)	157.7(9)	C(3)–C(4)–C(10)–C(5)	–166.0(2)
C(9)–C(1)–C(2)–C(3)	–51.0(4)	C(1')–C(4)–C(10)–C(9)	143.2(2)
N(1)–C(1)–C(2)–C(3)	74.7(5)	C(3)–C(4)–C(10)–C(9)	17.3(3)
C(1)–C(2)–C(3)–C(4)	64.2(4)	C(10)–C(4)–C(1')–C(2')	120.2(2)
C(2)–C(3)–C(4)–C(10)	–45.6(4)	C(3)–C(4)–C(1')–C(2')	–113.3(3)
C(2)–C(3)–C(4)–C(1')	–171.9(3)	C(10)–C(4)–C(1')–C(6')	–61.7(3)
C(10)–C(5)–C(6)–C(7)	0.9(5)	C(3)–C(4)–C(1')–C(6')	64.8(3)

Table 6. Continued

Torsion Angles/°			
C(5)–C(6)–C(7)–C(8)	–1.2(5)	C(6')–C(1')–C(2')–C(3')	0.1(3)
C(6)–C(7)–C(8)–C(9)	0.5	C(4)–C(1')–C(2')–C(3')	178.21(19)
C(7)–C(8)–C(9)–C(10)	0.5(4)	C(1')–C(2')–C(3')–C(4')	–0.1(3)
C(7)–C(8)–C(9)–C(1)	–178.4(3)	C(1')–C(2')–C(3')–C(3')	179.90(17)
C(2)–C(1)–C(9)–C(10)	22.1(3)	C(2')–C(3')–C(4')–C(5')	0.0(3)
N(1)–C(1)–C(9)–C(10)	–81.8(6)	Cl(3')–C(3')–C(4')–C(5')	180.0(2)
C(2)–C(1)–C(9)–C(8)	–159.0(3)	C(2')–C(3')–C(4')–Cl(4')	179.20(17)
N(1)–C(1)–C(9)–C(8)	97.0(6)	Cl(3')–C(3')–C(4')–Cl(4')	–0.8(3)
C(6)–C(5)–C(10)–C(9)	0.2(4)	C(3')–C(4')–C(5')–C(6')	0.1(4)
C(6)–C(5)–C(10)–C(4)	–176.5(3)	Cl(4')–C(4')–C(5')–C(6')	–179.1(2)
C(8)–C(9)–C(10)–C(5)	–0.9(3)	C(4')–C(5')–C(6')–C(1')	–0.1(4)
C(1)–C(9)–C(10)–C(5)	178.0(2)	C(2')–C(1')–C(6')–C(5')	0.0(4)
C(8)–C(9)–C(10)–C(4)	175.8(2)	C(4)–C(1')–C(6')–C(5')	–178.1(2)
C(1)–C(9)–C(10)–C(4)	–5.3(3)		

On the basis of the above crystal structure descriptions, the molecules in either the racemate or enantiomer have a similar backbone consisting of head, central, and tail three parts and are assembled in the same way. The significant differences between the racemate and enantiomer lie in conformation of the molecular tail structure, namely, the methylamine group. A thorough examination of detailed bond parameters summarized in Tables 5 and 6, respectively, reveals that the torsion angles of C1–N2–C3–C8 and C1–N2–C3–C4 in the racemate are 163.01° and –74.7°, while these of C9–C1–N1–C11 and C2–C1–N1–C11 in the enantiomer are –86.6° and 57.7°. The significant different torsion angles demonstrate the molecular tail structure differences. In both the racemate and enantiomer, identical chain-like hydrogen-bonding patterns are observed. One molecule acts as an acceptor for the other molecule which donates its proton. The molecules with identical chirality are related by hydrogen-bonding along the *b*-axis to form helical columns and paralleled columns are linked by van der Waals interactions.

It is generally believed that density of the crystal is the most important criterion to evaluate the relative stability between the racemate and enantiomer. The denser the crystal is, the more stable the crystal is.^{12,32} Density of sertraline racemate is higher than the enantiomer, and the hydrogen-bonding interactions connected the molecules in the racemate are stronger than those in the enantiomer based on the corresponding hydrogen bond distance. In addition, the disorder in the enantiomer may weaken a compact crystal packing in racemate. This evidence reveals that the racemate crystals are packed efficiently and are more stable than enantiomers, so the sertraline racemic mixture preferably crystallizes as a racemic compound rather than a conglomerate from the standpoint of molecular structure. These results are consistent with the conclusion drawn from the binary melting point phase diagram as well as DSC, PXRD, and FTIR analysis in the present work (Section 3.3).

4. Conclusions

The crystalline sertraline enantiomer was prepared, characterized, and compared with its hydrochloride salt in terms of solubility, hygroscopicity, and polymorphism propensity. Sertraline enantiomer is found to be less polymorphic than sertraline HCl salt, which provides an alternative formulation scheme. Although the solubility of free base is much lower than that of sertraline HCl salt, which is a disadvantage in formulation, it can be overcome by using the proper

formulation strategy and adopting novel drug delivery systems.

The crystalline sertraline racemate was obtained, and its solid-state nature was identified to be a racemic compound. The crystal structures of sertraline racemate and enantiomer are provided for the first time in the work. The racemate crystallizes in monoclinic $P12_1/n1$ space group, whereas the enantiomer crystallizes in monoclinic $P2_1$ space group. The comparison of crystal structures between the racemate and enantiomer confirm that the sertraline racemate is a racemic compound rather than conglomerate or pseudoracemate.

Acknowledgment. The authors gratefully acknowledge financial support of the Natural Sciences and Engineering Council of Canada through Individual Discovery and Strategic Grants. ApotexPharmaChem Inc. kindly supplied the API used in this study.

Supporting Information Available: The calculated and experimental XRPD patterns of sertraline racemate and sertraline enantiomer; XRPD patterns of starting solid and undissolved solid phase of sertraline enantiomers. This material is available free of charge via the Internet at <http://pubs.acs.org>.

References

- Zhou, M. X.; Foley, J. P. *J. Chromatogr. A* **2004**, *1052*, 13.
- (a) U.S. patent US005248699; (b) U.S. patent US2003055112; (c) U.S. patent US2001041815; (d) World patent WO0032551; (e) European patent EP0928784, (f) World patent WO0132601; (g) World patent WO0145692.
- (a) CA2594198; (b) U.S. patent US2008161607; (c) U.S. patent US2006229472; (d) World patent WO2006027658.
- Almarsson, O.; Hickey, M. B.; Peterson, M. L.; Morissette, S. L.; Soukasene, S.; McNulty, C.; Tawa, M.; MacPhee, J. M.; Remenar, J. F. *Cryst. Growth Des.* **2003**, *3*, 927.
- Remenar, J. F.; MacPhee, J. M.; Larson, B. K.; Tyagi, V. A.; Ho, J. H.; McIlroy, D. A.; Hickey, M. B.; Shaw, P. B.; Almarsson, O. *Org. Process Res. Dev.* **2003**, *7*, 990.
- Banerjee, P.; Bhatt, P. M.; Ravindra, N. V.; Desiraju, G. R. *Cryst. Growth Des.* **2005**, *5*, 2299.
- Chow, K.; Tong, H. H. Y.; Lum, S.; Chow, A. *J. Pharm. Sci.* **2008**, *97*, 2855.
- Bastin, R. J.; Bowker, M. J.; Slater, B. *J. Org. Process Res. Dev.* **2000**, *4*, 427.
- Lu, J.; Rohani, S. *Curr. Med. Chem.* **2009**, *16*, 884.
- Taber, G. P.; Pfisterer, D. M.; Colberg, J. C. *Org. Process Res. Dev.* **2004**, *8*, 385.
- Kozma, D. *CRC Handbook of Optical Resolutions via Diastereomeric Salt Formation*; CRC Press: Florida, 2002.
- Jacques, J.; Collet, A.; Wilen, S. *Enantiomers, Racemates and Resolutions*; John Wiley and Sons: New York, 1981.
- Wang, Y.; Chen, A. *Org. Process Res. Dev.* **2008**, *12*, 282.

- (14) Coquerel, G. Preferential Crystallization. *Top. Curr. Chem.* **2007**, *269*, 1.
- (15) Lorenz, H.; Sheehan, P.; Seidel-Morgenstern, A. *J. Chromatogr. A.* **2001**, *908*, 201.
- (16) Neau, S. H.; Shinwari, M. K.; Hellmuth, E. W. *Int. J. Pharm.* **1993**, *999*, 303.
- (17) He, Q.; Zhu, J.; Gomaa, H.; Jennings, M.; Rohani, S. *J. Pharm. Sci.* **2009**, *98*, 1835.
- (18) Zhang, G. Z.; Paspal, S.; Suryanarayanan, R.; Grant, D. J. W. *J. Pharm. Sci.* **2003**, *92*, 1356.
- (19) Lorenz, H.; Seidel-Morgenstern, A. *Thermochimica* **2004**, *415*, 55.
- (20) Bernstein, J. *Polymorphism in Molecular Crystals*; Clarendon Press: Oxford, 2002.
- (21) Kitamura, M. *Cryst. Growth Des.* **2004**, *4*, 1153.
- (22) Aaltonen, J.; Alles, M.; Mirza, S.; Koradia, V.; Gordon, K.; Rantanen, J. *Eur. J. Pharm. Biopharm.* **2009**, *7*, 23.
- (23) Mullin, J. W. *Crystallization*; Butterworth Heinemann Ltd: Oxford, 1993.
- (24) Chen, S.; Xi, H.; Yu, L. *J. Am. Chem. Soc.* **2005**, *127*, 17439.
- (25) Ostwald, W. *Z. Phys. Chem.* **1897**, *22*, 289.
- (26) McCrone, W. C. *Polymorphism*, In *Physics and Chemistry of the Organic Solid State*; Fox, D., Labes, M. M., Weissberger, A., Eds.; Wiley-Interscience: New York, 1965; Vol. 2, p 725.
- (27) Roy, S.; Aitipamula, S.; Nangia, A. *Cryst. Growth Des.* **2009**, *5*, 2261.
- (28) Kesisoglou, F.; Panmai, S.; Wu, Y. H. *Adv. Drug Delivery Rev.* **2007**, *59*, 631.
- (29) Jannin, V.; Musakhanian, J.; Marchaud, D. *Adv. Drug Delivery Rev.* **2008**, *60*, 6,734.
- (30) Constantinides, P. P.; Tustian, A.; Kessler, D. R. *Adv. Drug Delivery Rev.* **2004**, *56*, 1243.
- (31) Kaemmerer, H.; Lorenz, H.; Black, S. N.; Seidel-Morgenstern, A. *Cryst. Growth Des.* **2009**, *9*, 1851.
- (32) Brock, C. P.; Schweizer, W. B.; Dunitz, J. D. *J. Am. Chem. Soc.* **1991**, *113*, 9811.